(11) J. J. Ziolkowski, private communication, 1969.
(12) C. L. Angell, F. A. Cotton, B. A. Frenz, and T. R. Webb, *J. Chem. Soc., Chem. Commun.*, 399 (1973).
(13) F. A. Cotton, B. A. Frenz, and T. R. Webb, *J. Amer. Chem. Soc.*, **95**, 4431 (1973).
(14) F. A. Cotton, B. G. Deboer, M. D. Laprade, J. R. Pipal, and D. A. Ucko, *J. Amer. Chem. Soc.*, **92**, 2926 (1970).
(15) K. G. Caulton and F. A. Cotton, *J. Amer. Chem. Soc.*, **91**, 6517 (1969); F. A. Cotton, *Accounts Chem. Res.*, **2**, 240 (1969).
(16) V. I. Belova and Z. S. Dergacheva, *Russ. J. Inorg. Chem.*, **16**, 1626 (1971).
(17) **Note Added in Proof.** We regret having failed to notice the paper by R. D. Cannon and J. L. Tong, *Nature*, **216** 681 (1967), in which the carbonato analog of $Cr_2(OAc)_4$ is described.

Contribution from the Chemistry Department,
University of Virginia, Charlottesville, Virginia 22901

Infrared and Raman Studies of Alkali Metal Atom Matrix Reactions with Fluorine. Vibrational Spectrum of the $M^+F_2^-$ Species

WILMONT F. HOWARD, Jr. and LESTER ANDREWS*

Received August 9, 1974 AIC405572

Argon matrix reactions of alkali metal atoms with fluorine have been studied using laser Raman and infrared spectroscopy. Raman signals appropriate for the ν_1 intraionic $(F \leftrightarrow F)^-$ mode in the $M^+F_2^-$ species have been observed to show an alkali metal effect due to interaction with the ν_2 interionic $M^+ \leftrightarrow F_2^-$ mode. Infrared spectra revealed several ν_2 assignments for the $M^+F_2^-$ molecules and intense sharp bands due to the MF and $(MF)_2$ species.

Introduction

The fluorine molecular anion, F_2^-, was first observed in radiation-damaged salts by electron spin resonance spectroscopy. In 1955, Känzig[1] postulated the existence of F_2^- in γ-irradiated LiF at 77°K. In later work, Delbecq, *et al.*[2], reproduced the Känzig results on F_2^-, while Vande Kieft and Gilliam[3] produced the F_2^- species by irradiation of alkali metal bifluoride salts ($M^+HF_2^-$). Balint-Kurti and Karplus[4] have performed potential energy surface calculations for the reaction

$$Li + F_2 \rightarrow LiF_2 \rightarrow LiF + F \quad (1)$$

Even though this reaction is exothermic by approximately 100 kcal/mol, there is a stable intermediate, isosceles triangular $Li^+F_2^-$, which has a maximum calculated well depth of about 40 kcal/mol. Recently, Ham and Chang[5] have attributed the chemiluminescence arising from dilute gas mixtures of sodium and fluorine to NaF_2. Very recently, Martinez de Pinillos and Weltner[6] have obtained electron spin resonance evidence for F_2^- from alkaline earth metal atom–F_2 matrix reactions.

The possibility of observing such a potentially unstable intermediate species as $M^+F_2^-$ was greatly enhanced by the stabilizing effect of an Ar matrix. The reaction intermediate produced during condensation of alkali atoms and F_2 was trapped in the rare gas lattice and kept available for spectroscopic examination. This provided a look at the mechanism of an elementary chemical reaction, the combination of two elements to form the alkali halide molecule. Here follows a detailed vibrational spectroscopic study of alkali metal atom–molecular fluorine matrix reactions.

Experimental Section

The 15°K cryogenic refrigeration and vacuum apparatus for infrared[7,8] and Raman[9,10] studies of alkali metal atom matrix reactions has been described previously. The techniques for handling the alkali metals for producing atomic beams have also been reported. Evaporation temperatures appropriate to 0.5–1.0 μ of alkali metal vapor pressure were used.[8]

Fluorine was handled in a passivated stainless steel vacuum system constructed with "swaglok" fittings and Nupro SS-4BK valves. Pressures were measured with an Ashcroft vacuum gauge with a stainless steel Bourdon tube. Fluorine (Allied Chemical) obtained from the Naval Research Laboratory in small stainless steel cans was passed through a stainless steel U tube immersed in liquid nitrogen before use. In some cases the F_2 can was cooled to 77°K before the sample was withdrawn. Argon (Air Products, 99.995%) matrix samples were prepared using standard techniques.[11]

For infrared experiments, gas spray-on rates were initially 1 mmol/hr slowly increasing to 2 mmol/hr when alkali metal atom codeposition was started. Sample formation was monitored by infrared survey scans and stopped after 10–20 hr when the sample transmission reached 30–40%. Calibration spectra, run at 8 or 3.2 cm^{-1}/min on a Beckman IR-12 filter–grating spectrophotometer, are accurate to ± 0.5 cm^{-1}.

Raman experiments employed gas deposition for 3–5 hr at 3 mmol/hr with metal atoms for all but the first hour. Raman spectra were recorded on a Spex Ramalog using Coherent Radiation Model 52G argon and krypton ion lasers. Dielectric filters (Corion Instrument Corp.) were used to remove undesired laser plasma emission from recorded spectra. Raman signals were calibrated by superimposing emission lines on each side of the band during an actual running scan, which gives an accuracy of 0.5 to 1.0 cm^{-1} depending upon the half-bandwidth.

Results

The infrared and Raman spectra of each alkali metal–fluorine–argon matrix combination will be treated in turn. The Ar–F_2 samples were diluted 50:1 for Raman studies and 100:1 for infrared experiments, unless otherwise stated. As expected, the frequency regions for alkali fluorides trapped in solid argon were void of signals in the Raman work. The Raman signals shifted about 460 cm^{-1} were unstable with respect to laser photolysis; the Na–F_2 reaction intermediate, which had a half-life of approximately 25 min, was the most photolytically stable new species observed. Further, these signals exhibited faster degradation than the 892-cm^{-1} F_2 band, which has been shown to undergo photolytic dissociation with the blue Ar^+ laser lines and to react in solid Kr and Xe to form KrF_2 and XeF_2, respectively.[12]

The infrared spectra were unexpectedly complex due to fluorine-carried impurities and alkali fluoride aggregates. Impurity bands will be identified where possible in the appropriate tables but will otherwise not be mentioned. Infrared surveys were taken with purified and unpurified F_2 in the matrix without alkali metal, which provided a check on the impurity signals.

Lithium. Raman spectra involving either Li isotope yielded identical signals, within experimental error: the F_2 signal shifted 892.2 ± 0.5 cm^{-1} from the laser source and a band of moderate intensity at 452.0 ± 1.0 cm^{-1} (^6Li) or 451.6 ± 0.8 cm^{-1} (^7Li). This band is contrasted in Figure 1 with the analogous signals produced by the other alkali metal species. No other band was observed in any Li–F_2 Raman experiment.

The infrared scans of ^6Li–F_2 reaction products showed a strong doublet at 891.8 (0.32) and 886.6 cm^{-1} (0.53) (optical

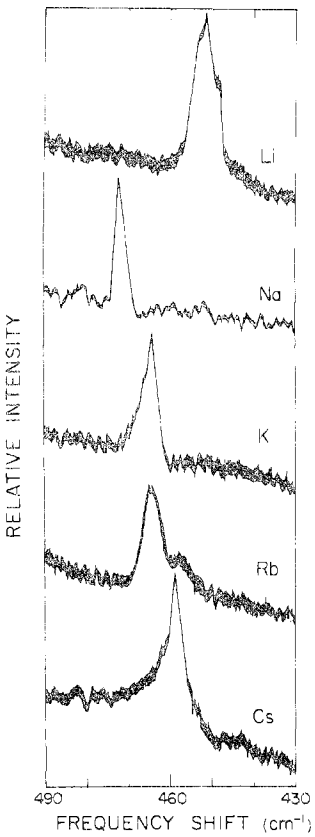

Figure 1. Raman signals in the 460-cm^{-1} region from alkali metal–fluorine matrix reactions. Conditions: 100 mW of 4880-Å excitation at the sample, 10 cm^{-1}/min scan speed, 0.3 × 10^{-9} A range, 3 sec rise time (except Na), 10 sec rise time (Na); 5-Å dielectric spike and neutral density filters used.

density values will be given parenthetically, as here), which were shifted to 841.0 (0.27) and 836.5 cm^{-1} (0.44) in ^{7}Li work (M/R = 50), both illustrated in Figure 2. A moderately intense signal at 708.4 cm^{-1} (0.25) found in ^{6}Li experiments had no observable ^{7}Li counterpart, presumably due to masking by the CO_2 impurity present at 663.5 cm^{-1} (0.54); the former signal was completely destroyed with matrix warming to 38°K and subsequent diffusion.

Other LiF species (dimers and higher aggregates) were observed which exhibited isotopic shifts, and some mixed lithium species were found in a $^{6,7}Li$ trial. A multiplet at 585.7 (0.10), 576.5 (0.17), 569.8 (0.20), and 562.4 cm^{-1} (0.16) observed with the lighter isotope was found at 556.0 (0.12), 550.7 (0.16), and 538.4 cm^{-1} (0.16) with ^{7}Li. A ^{6}Li doublet at 519.8 (0.06) and 509.2 cm^{-1} (0.10) was shifted to 499.1 (0.06) and 484.6 (0.11) with ^{7}Li. The diffusion experiment with ^{6}Li mentioned above eliminated the 890-cm^{-1} doublet but preserved the lower frequency features around 570 and 515 cm^{-1}, although they appeared with lower intensity. Table I lists the infrared absorptions observed in all of the alkali metal–F_2 matrix reaction studies.

A trial with mixed Li isotopes showed both LiF monomer signals with comparable intensities and indicated a ^{6}Li:^{7}Li ratio of 3:4. The series of bands in the 540–585-cm^{-1} region was present, although not as well defined as in earlier trials, and a previously unobserved band at 560.2 cm^{-1} (0.10) was found. The band clustered around 500 cm^{-1} appeared with an intermediate member at 510.1 cm^{-1} (0.05); the signals previously found at 520 and 499 cm^{-1} were too weak to measure. Evidence of lithium superoxides was found in all Li experiments.[13]

Sodium. The Raman signal observed at 474.9 ± 0.5 cm^{-1} in Na–F_2 trials was stronger relative to the F_2 band than with any of the other alkali metals; the sodium spectrum is shown

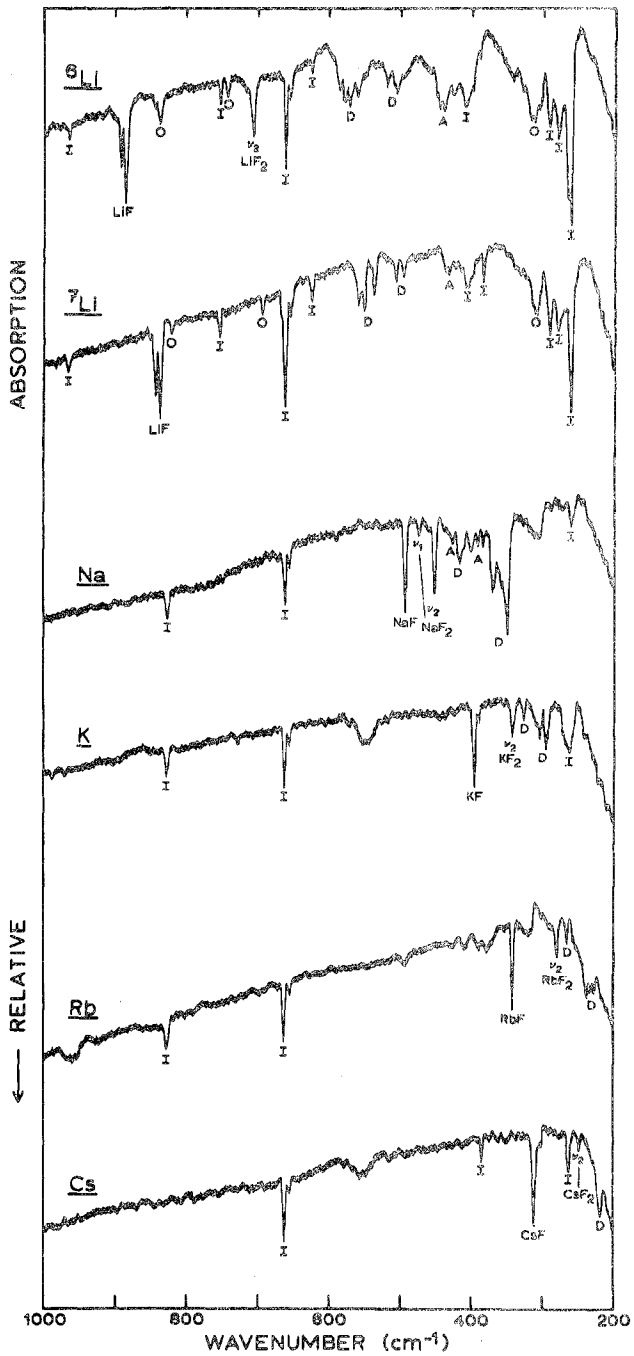

Figure 2. Infrared spectra of alkali metal–fluorine reaction products suspended in an Ar matrix; spectral region 200–1000 cm^{-1}, M/R = 100, scan speed 40 cm^{-1}/min, 4.5% gain. Legend: I, impurity; O, oxides; D, dimer; A, aggregate.

in Figures 1 and 3. The success of this experiment prompted two others, one with Ar:Cl_2 = 100:1 and the other with Ar:Cl_2:F_2 = 400:1:2; the resulting spectra are compared in Figure 3. Molecular chlorine appeared at 538 ± 1 cm^{-1}, with a $^{35}Cl^{37}Cl$ counterpart at 530 ± 1 cm^{-1} and metal-associated features at 275.0 ± 0.5 and 225.0 ± 0.5 cm^{-1}, while the mixed-halogen trial yielded no new bands but did reproduce the signals already mentioned.

The infrared spectrum of Na–F_2 matrix reaction products showed several signals, with the highest frequency band appearing at 492.6 cm^{-1} (0.64). The Na–F_2 Raman band was reproduced in the infrared spectrum at 475.4 cm^{-1} (0.10), with a stronger partner at 453.6 cm^{-1} (0.38). Dimer features were noted at 417.2 (0.19), 370.8 (0.60), 359.4 (0.12), and 350.3

Table I. Band Positions and Assignments from Infrared Spectra of Matrix-Trapped Alkali Metal–Fluorine Reaction Products

Freq, cm^{-1}		
$^6Li + F_2$	$^7Li + F_2$	Assignment
965.5	965.7	ν_2 OCF_2
891.8, 886.6	841.0, 836.5	LiF
839.7	815.3	ν_5 LiO_2Li
769.4	769.6	ν_6 OCF_2
743.4	698.3	ν_2 LiO_2
708.4		ν_2 LiF_2
663.5, 658.0	663.2, 657.7	ν_2 CO_2
613.8	613.5	ν_5 OCF_2
585.7, 576.5, 569.8, 562.4	556.0, 550.7, 538.4	ν_5 $(LiF)_2$
519.8, 509.2	499.1	$(LiF)_2$
447.4, 438.0	427.4, 420.1	$(LiF)_x$ (?)
413.5	413.2	Impurity
	385.3	ν_4 SiF_4
314.0	297.7	ν_4 LiO_2Li
290.9, 281.0, 262.4	291.1, 280.7, 262.0	Impurity

$Na + F_2$		$K + F_2$	
Freq, cm^{-1}	Assignment	Freq, cm^{-1}	Assignment
826.2	ν_3 OF_2	825.9	ν_3 OF_2
663.6, 658.0	ν_2 CO_2	663.8, 657.8	ν_2 CO_2
492.6	NaF	396.6, 391.6	KF
475.4	ν_1 NaF_2	342.2	ν_2 KF_2
453.6	ν_2 NaF_2	328.5	$(KF)_2$–linear
426.3	$(NaF)_x$	303.7	$(KF)_2$–cyclic
417.2	$(NaF)_2$–linear	294.2	$(KF)_2$–linear
401.3, 391.3, 382.8	$(NaF)_x$	280.6	$(KF)_2$–cyclic
370.8	$(NaF)_2$–cyclic		
359.4	$(NaF)_2$–linear		
350.3	$(NaF)_2$–cyclic		
273.1	(?)		

$Rb + F_2$		$Cs + F_2$	
Freq, cm^{-1}	Assignment	Freq, cm^{-1}	Assignment
826.4	ν_3 OF_2	663.3, 658.1	ν_2 CO_2
663.4, 658.2	ν_2 CO_2	385.2	ν_4 SiF_4
332.2	RbF	312.2	CsF
266.1	ν_2 RbF_2	262.1	Metal fluoride (?)
254.4, 236.8, 233.2, 231.6, 228.8	$(RbF)_2$	248.3	ν_2 CsF_2
		214.5	$(CsF)_2$

cm^{-1} (completely absorbing), while weaker polymer bands were found at 426.3 (0.06), 401.3 (0.10), 391.3 (0.06), and 382.8 cm^{-1} (0.09). The intense red color of Na metal rendered the sample visually opaque before the experiment was terminated.

Potassium. A band at 464.1 ± 0.7 cm^{-1} was the only signal noted in K–F_2 Raman trials, other than the F_2 feature at 892 cm^{-1}. The infrared study, on the other hand, yielded seven bands associated with K–F species. The strongest feature of these spectra was a doublet at 396.6 (0.84) and 391.6 cm^{-1} (0.29). Lower frequency signals included two isolated bands at 342.2 (0.11) and 328.5 cm^{-1} (0.05) and a triplet at 303.7 (0.11), 294.2 (0.19), and 280.6 cm^{-1} (0.26).

Rubidium. Spectra obtained from Rb–F_2 reaction products were relatively uncomplicated. The lower frequency Raman signal was found at 462.4 ± 0.7 cm^{-1} and was the most photolytically unstable band in this series. The highest frequency infrared feature was noted at 332.2 cm^{-1} (0.39), while other signals included a doublet at 266.1 (0.12) and 254.4 cm^{-1} (0.08) and a quartet at 236.8 (0.20), 233.2 (0.15), 231.6 (0.16), and 228.8 cm^{-1} (0.13).

Cesium. The vibrational spectra of Cs–F species showed a band at 458.8 ± 0.5 cm^{-1} in the Raman scan illustrated in Figure 1, while three new features appeared in the infrared spectrum shown in Figure 2 at 312.2 (0.54), 248.3 (0.09), and 214.5 cm^{-1} (0.13).

Discussion

The Raman frequency of molecular F_2 is in nearly exact agreement with the gas-phase value[14] but is shifted 3 cm^{-1} from the fundamental crystal vibration which appeared at 895 cm^{-1}.[15] This is indicative of the low degree of aggregate formation (*i.e.*, intermolecular fluorine bonding) which occurs during sample condensation, in contrast to the extensive clustering noticed with heavier halogens.[16]

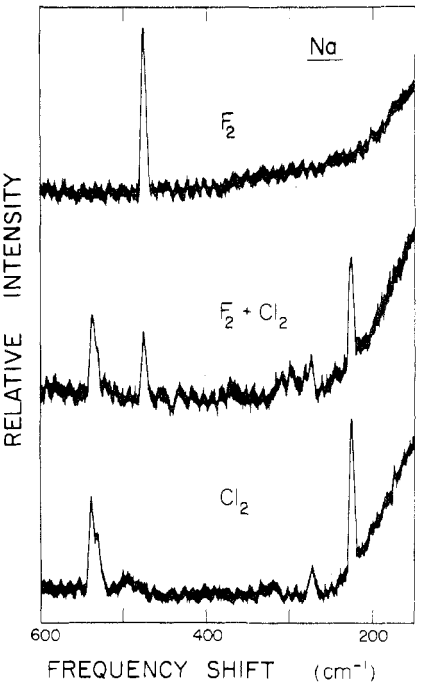

Figure 3. Raman spectra of matrix F_2 and Cl_2 reactions with Na atoms. Parameters: Ar:F_2 = 50:1, 5-Å dielectric and neutral density filters, 45 mw of 4880-Å excitation, 0.1 × 10^{-9} A range, rise time 3 sec; Ar:F_2:Cl_2 = 400:3:1, 5-Å dielectric filter, 250 mW of 5145-Å excitation, 0.1 × 10^{-9} A range, 10 sec rise time; Ar:Cl_2 = 100:1, 5-Å dielectric filter, 0.3 × 10^{-9} A range, 150 mW of 4880-Å excitation, 3 sec rise time. All scan speeds were 20 cm^{-1}/min.

Table II. Vibrational Assignments to the Symmetric Modes of the $M^+F_2^-$ Species which Is Assumed to Have Triangular Geometry

Species	ν_1, cm^{-1}	ν_2, cm^{-1}	Species	ν_1, cm^{-1}	ν_2, cm^{-1}
$^6Li^+F_2^-$	452	708	$K^+F_2^-$	464	342
$^7Li^+F_2^-$	452		$Rb^+F_2^-$	462	(266)[a]
$Na^+F_2^-$	475	454	$Cs^+F_2^-$	459	(248)[a]

[a] Observed bands; however $(MF)_2$ assignments cannot be ruled out.

The Raman bands observed near 460 cm^{-1} following alkali metal atom–molecular fluorine reactions have been attributed to the intraionic $(F–F)^-$ vibration in the $M^+F_2^-$ species.[17] The Raman study of Cl_2 as a pseudoisotope of F_2 represented in Figure 3 confirms that the 475-cm^{-1} $Na^+F_2^-$ band arises from a two-halogen-atom species. $Na^+Cl_2^-$ produced an analogous signal at 225 cm^{-1} and the mixed F_2–Cl_2 run yielded only the same two signals without intermediate components, which indicates that these bands originate from diatomic, rather than triatomic, halogen species. Table II contrasts the vibrational assignments for five $M^+F_2^-$ species.

Interpretation of the infrared spectra of alkali metal fluoride species was made in comparison with earlier works dealing with matrix-trapped lithium, sodium, and potassium fluorides produced by Knudsen cell effusion of the salt.[18,19] Similar studies with RbF and CsF have, as yet, not been done, and assignments of spectral bands from Rb– and Cs–F work are less certain. Comparison of the several reaction product spectra to the blank (no metal) F_2 scans eliminated mislabeling of impurity signals.

Table III contrasts gas-phase and matrix-isolated alkali metal fluoride vibrational frequencies. Signal positions were

Table III. Gas-Phase and Matrix-Isolated Frequencies of Alkali Metal Fluorides

Molecule	Gas-phase freq, cm^{-1}	Matrix-isolated freq, cm^{-1}: Knudsen cell salt effusion	Matrix-isolated freq, cm^{-1}: Alkali metal–fluorine reaction
^6LiF	945.0[a]	886[e]	886.6[g]
^7LiF	894.0[a]	838[e]	836.5
NaF	529 ± 2[b]	495.5[f]	492.6
KF	429 ± 3[b]	397[f]	396.6
RbF	376 ± 4[c]		332.2
CsF	349.3[d]		312.2

[a] E. F. Pearson and W. Gordy, *Phys. Rev.*, 177, 52 (1969). [b] Reference 18. KF shows ω_e value. [c] ω_e value from ref 19. [d] Reference 20. [e] M. J. Linevsky, *J. Chem. Phys.*, 38, 658 (1963). [f] Reference 17. [g] This work.

red-shifted from 5.9% (KF) to 10.8% (CsF), as usually noted for ionic species; this frequency change arises from extensive dipole–induced dipole interactions. The lighter fluorides (Li, Na, K) were assigned by comparison to spectra from the salt effusion studies[18,19] while the frequencies for RbF and CsF were determined by contrasting gas-phase data[20–22] and the expected matrix shift.

Dimer and higher polymer formation has been noted with alkali metal fluorides, and infrared signal assignments have been made.[18,19] Comparison with the results attained here showed that dimer formation was favored over aggregation, even at very high metal concentrations relative to F_2. Further, it appeared from a comparison of band intensities that the cyclic dimer was slightly preferred over the linear form. A few of the weaker bands present in the Knudsen cell–salt effusion experiments with LiF and KF exhibited signal merging in this study, and only one signal was found at the approximate mean of the previously recorded frequencies. With the exception of the coalesced signals, frequency agreement with the earlier studies was excellent, with deviations usually less than 2 cm^{-1}.

The first step in the assignment of a band to ν_2, the interionic mode of the presumably isosceles triangular MF_2 molecule, was a consideration of the position of the highest frequency cyclic dimer frequency. This vibration, a B_{3u} mode in the D_{2h}-symmetry species, is represented by A, while B illustrates ν_2 of the triangular intermediate and C shows a simple monomer vibration. The progression and vibrational similarity of these three modes was striking and immediately suggested that the frequency of B would be intermediate to those of A and C but likely closer to the dimer band.

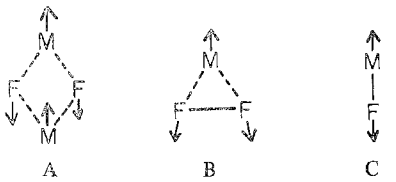

A B C

A further consideration was the possible interionic vibrational similarities between $M^+F_2^-$ and $M^+O_2^-$. Since ν_1 and ν_2 of these species are both a_1 modes, there will be mode mixing, and the position of the Raman-active intraionic stretch will be influenced by the frequency of ν_2, the interionic vibration. It is probable that the interionic frequencies of $M^+O_2^-$ and $M^+F_2^-$ are similar: these signals appear at 699, 391, 307, 255, and 236 cm^{-1} for the Li^+, Na^+, K^+, Rb^+, and Cs^+ superoxides, respectively.[13,23–25] This approach predicted a frequency crossover of the interionic and intraionic modes between Li and Na, and since interactions of this type force vibrational frequencies apart, this model predicted that the lowest ν_1 value for $M^+F_2^-$ would be obtained with the Li cation and the highest with Na^+, as was observed. Values for the intraionic frequencies with the heavier cations were expected to decrease regularly, and this was also found.

Analyses of the infrared spectra in light of the above arguments led to the ν_2 assignments of $^6Li^+F_2^-$, $Na^+F_2^-$, and $K^+F_2^-$ at 708.4, 453.6, and 342.2 cm^{-1}, respectively. If the assumption is made that the species assumed a diatomic character (*i.e.*, the metal vibrates against a 38-amu atom), a simple isotopic frequency calculation suggested that ν_2 of $^7Li^+F_2^-$ would absorb at 663.3 cm^{-1}, but this region was obscured by the strong signal of CO_2, which was desorbed from the metal upon heating. An identical calculation with ν_2 of $Li^+O_2^-$ deviated by only 1.2 cm^{-1} from the observed value. The appearance of the band at 475.4 cm^{-1} in the Na–F_2 infrared trial, in agreement with the Raman measurement, was attributed to interaction between the symmetric interionic and intraionic vibrations, where the intensity of the weaker ν_1 infrared signal was enhanced by the proximity of the stronger ν_2 band. No duplication of the ν_1 Raman signal was observed with any other cation.

Since no results on RbF and CsF salt effusion have been published, definite assignment of the lower alkali metal fluoride bands in the Rb–Cs–F_2 spectra was curtailed. However, in view of the ν_2 $M^+F_2^-$ positions relative to the dimer bands of the lighter metal fluorides, the highest frequency bands beneath the monomer vibrations were tentatively attributed to ν_2 of $Rb^+F_2^-$ (266.1 cm^{-1}) and $Cs^+F_2^-$ (248.3 cm^{-1}), while signals below these frequencies are likely due to dimers.

Since the electron transferred from the alkali metal to the fluorine molecule enters an antibonding σ orbital, the net bond order is reduced from 1 to $^1/_2$. A casual approximation of the F_2^- vibrational frequency would be half that of F_2, and it was gratifying to note that the assigned frequency falls near 50% of the F_2 fundamental.

Subsequent studies of alkali metal reactions with simple halogens have revealed that the addition of an antibonding electron to the halogen red-shifted the absorption curve of the molecule.[26] This alteration was quite extensive and suggested that the absorption maximum of F_2 at 2900 Å[27] would be in the near-ultraviolet region for F_2^-. At any rate, the intensity of the F_2^- Raman band was stronger than might be expected, and this is tentatively attributed to a preresonance enhancing of the Raman signal strength.

Conclusions

The intraionic and interionic modes (ν_1 and ν_2, respectively) of $M^+F_2^-$ have been identified and calibrated, and the effect of mode mixing on the vibrational frequency of ν_1 has been discussed. In addition, contrasts were drawn between gas-phase and matrix-isolated MF stretching frequencies, and comparisons of $(MF)_x$ production between alkali metal–halogen reactions and Knudsen cell salt effusion were made, which assisted in infrared band assignments. Finally, the red displacement of the absorption spectra of F_2^- relative to F_2 yielded the possibility of preresonance Raman intensity enhancement, and the comparative vibrational frequencies of the F_2 and F_2^- species corresponded to a rough molecular orbital prediction.

Acknowledgment. The authors gratefully acknowledge financial support for this research by the National Science Foundation under Grant GP-38420X and an Alfred P. Sloan fellowship for Lester Andrews. We thank Dr. W. B. Fox for the fluorine samples and his helpful suggestions on handling fluorine.

Registry No. F_2, 7782-41-4; ^6Li, 14258-72-1; ^7Li, 13982-05-3; Na, 7440-23-5; K, 7440-09-7; Rb, 7440-17-7; Cs, 7440-46-2; $^6Li^+F_2^-$, 53369-60-1; $^7Li^+F_2^-$, 53369-61-2; $Na^+F_2^-$, 39327-45-2; $K^+F_2^-$, 39327-43-0; $Rb^+F_2^-$, 39327-46-3; $Cs^+F_2^-$, 11093-73-5; ^6LiF, 14885-65-5; ^7LiF, 17409-87-9; NaF, 7681-49-4; KF, 7789-23-3; RbF,

13446-74-7; CsF, 13400-13-0; $(LiF)_2$, 12265-82-6; $(NaF)_2$, 12285-64-2; $(KF)_2$, 12285-62-0; $(RbF)_2$, 37279-33-7; $(CsF)_2$, 12285-54-0.

References and Notes

(1) W. Känzig, *Phys. Rev.*, **99**, 1890 (1955).
(2) C. J. Delbecq, W. Hayes, and P. H. Yuster, *Phys. Rev.*, **121**, 1043 (1961).
(3) J. L. Vande Kieft and O. R. Gilliam, *Phys. Rev. B*, **1**, 2015 (1970).
(4) G. G. Balint-Kurti and M. Karplus, *Chem. Phys. Lett.*, **11**, 203 (1971); *J. Chem. Phys.*, **50**, 478 (1969).
(5) D. O. Ham and H. W. Chang, *Chem. Phys. Lett.*, **24**, 579 (1974).
(6) J. V. Martinez de Pinillos and W. Weltner, Jr., personal communication, 1974.
(7) L. Andrews, *J. Chem. Phys.*, **48**, 972 (1968).
(8) R. C. Spiker, Jr., and L. Andrews, *J. Chem. Phys.*, **59**, 1851 (1973).
(9) D. A. Hatzenbühler and L. Andrews, *J. Chem. Phys.*, **56**, 3398 (1972).
(10) L. Andrews and R. C. Spiker, Jr., *J. Chem. Phys.*, **59**, 1863 (1973).
(11) W. F. Howard, Jr., M.S. Thesis, University of Virginia, Charlottesville, Va., 1974.
(12) W. F. Howard, Jr., and L. Andrews, *J. Amer. Chem. Soc.*, in press.
(13) L. Andrews, *J. Chem. Phys.*, **50**, 4288 (1969).
(14) D. Andrychuk, *J. Chem. Phys.*, **18**, 233 (1950).
(15) T. M. Niemczyk, R. R. Getty, and G. E. Leroi, *J. Chem. Phys.*, **59**, 5600 (1973).
(16) W. F. Howard, Jr., and L. Andrews, *J. Raman Spectrosc.*, in press.
(17) W. F. Howard, Jr., and L. Andrews, *J. Amer. Chem. Soc.*, **95**, 3045 (1973).
(18) A. Snelson and K. S. Pitzer, *J. Phys. Chem.*, **67**, 882 (1963).
(19) Z. K. Ismail, R. H. Hauge, and J. L. Margrave, *J. Inorg. Nucl. Chem.*, **35**, 3201 (1973).
(20) R. K. Ritchie and H. Lew, *Can. J. Phys.*, **42**, 43 (1964).
(21) V. I. Baikov and K. P. Vasilevskii, *Opt. Spektrosk.*, **22**, 364 (1967).
(22) S. E. Veasey and W. Gordy, *Phys. Rev. A*, **138**, A1303 (1965).
(23) L. Andrews, *J. Phys. Chem.*, **73**, 3922 (1969).
(24) L. Andrews, *J. Chem. Phys.*, **54**, 4935 (1971).
(25) L. Andrews, J.-T. Hwang, and C. Trindle, *J. Phys. Chem.*, **77**, 1065 (1973).
(26) W. F. Howard, Jr., and L. Andrews, *J. Amer. Chem. Soc.*, **95**, 2056 (1973). The Cl_2^- maximum depending upon the host is 3400–3600 Å whereas Cl_2 itself peaks near 3300 Å. See also Figure 3-30 in J. G. Calvert and J. N. Pitts, Jr., "Photochemistry," Wiley, New York, N. Y., 1966.
(27) R. K. Steunenberg and R. C. Vogel, *J. Amer. Chem. Soc.*, **78**, 901 (1956).

Contribution from the Department of Chemistry,
Eastern Michigan University, Ypsilanti, Michigan 48197

Mechanism of the Permanganate Ion Oxidation of Vanadium(IV)

FRED M. MOORE and KENNETH W. HICKS*

Received January 10, 1974 AIC40018X

The reduction of the permanganate ion by oxovanadium(IV) in perchloric acid solutions was determined using stopped-flow spectrophotometric techniques. The rate expression $-d[MnO_4^-]/dt = (k_0 + k_1[H^+])[MnO_4^-][VO^{2+}]$, where $k_0 = 72.9 \pm 1.6\ M^{-1}\ sec^{-1}$ and $k_1' = 28.8 \pm 1.7\ M^{-2}\ sec^{-1}$, was found to represent the reaction at 526 nm at 25.0°, $[H^+] = \mu = 1.00$. The form of the rate expression, the observation of a transient intermediate ($\lambda_{max} \sim 410$ nm), and thermodynamic parameters $\Delta H^{\ddagger} = 10.8 \pm 0.5$ kcal/mol and $\Delta S^{\ddagger} = -12.9 \pm 1.9$ eu give indication for a mechanism in which there is complex formation.

The reaction between the permanganate ion, MnO_4^-, and the vanadium(IV) ion, VO^{2+}, in acid media was investigated as part of a series of permanganate ion oxidations of inorganic ions in an effort to elucidate the conditions necessary for the occurrence of the two-electron reduction pathway for the MnO_4^- ion.[1] The reaction between the permanganate ion, MnO_4^-, and various metal ions, $Fe(phen)_3^{2+}$,[2] $Fe(CN)_6^{4-}$,[3] and $Mo(CN)_8^{4-}$,[1] have been shown to occur *via* an outer-sphere, one-electron-transfer process. The reactions are classified as outer sphere from their observed rate laws and the reasonable agreement with rate constants obtained from the Marcus theory.[4] The reaction between VO^{2+} and MnO_4^- is also of interest in that protons are produced in the overall reaction

$$MnO_4^- + 5VO^{2+} + H_2O \rightarrow Mn(II) + 5VO_2^+ + 2H^+$$

whereas in the majority of reactions involving the reduction of the permanganate ion, protons are consumed. It has been observed that when the oxidation half-cell reaction of the reductant is less than +0.56 V, the value for the MnO_4^-–MnO_4^{2-} couple, the reaction proceeds without the aid of a proton. However, when the oxidation half-cell reaction is more negative than −0.56 V, the reaction proceeds with a direct proton dependence.[5]

A two-electron-transfer step accompanied by the formation of a transient intermediate has been observed for several MnO_4^-–organic systems[6-8] with the reduced manganese species characterized as Mn(V). This pathway was shown to be operative in the reaction of the bromide ion, Br^-, with MnO_4^-.

Kriss and Yatsimirskii reported experiments performed in sulfuric acid involving the VO^{2+}–MnO_4^- reaction in which they observed an induction period in the disappearance of the permanganate ion and postulated the presence of Mn(III) as a stable reaction product.[9] Rosseinsky and Nicol also reported a study of this reaction performed in $HClO_4$ in which they found the stoichiometry to vary from 2.5 to 4.7 depending upon the reaction conditions.[10] We report herein experiments which provide a somewhat different interpretation.

Experimental Section

A stock solution of potassium permanganate was prepared by dissolving Baker Analyzed reagent grade $KMnO_4$ in distilled water, boiling the solution, and standardizing against As_2O_3 after a fine glass frit filtration to remove MnO_2. The solution was stored in a dark bottle away from light and restandardized periodically. Perchloric acid solutions were prepared by dilution of concentrated $HClO_4$ with permanganate-distilled, ion-exchanged water and were standardized against NaOH solutions. Stock solutions of $NaClO_4$ were prepared by the addition of recrystallized reagent grade Na_2CO_3 to $HClO_4$ solutions of known concentration. The remaining hydrogen ion concentration was determined by titration against NaOH. Vanadium(IV) perchlorate stock solutions were prepared by two methods: (1) by the addition of a stoichiometric amount of $Ba(ClO_4)_2$ to a solution of $VOSO_4$ dissolved in 0.1 *M* $HClO_4$; $BaSO_4$ was removed by centrifugation; (2) by the electrolytic reduction of a slurry of V_2O_5 at platinum electrodes in 0.1 *M* $HClO_4$. Both solutions gave similar kinetic results. Total vanadium content was determined spectrophotometrically as the V^V–H_2O_2 complex[11] and [V(IV)] was determined spectrophotometrically at its maximum absorbance (λ_{max} 760 nm, ϵ 17.1 $M^{-1}\ cm^{-1}$).[12]

Kinetic Studies. The kinetics of the reaction were determined using an Aminco-Morrow stopped-flow apparatus attached to a Beckman DU monochromator. The progress of the reaction was observed at 526 nm, where MnO_4^- is the only absorbing species, and at 410 nm. The output from the photomultiplier was monitored by a Tektronic Model 564 storage-type oscilloscope and the stored trace recorded with a Polaroid camera. Apparent pseudo-first-order ($[VO^{2+}]_0 \gtrsim 25[MnO_4^-]_0$) and second-order rate constants were calculated from absorbance–time data using both a linear least-squares program and graphical techniques.

Ionic strength was maintained at 1.00 *M* in most experiments by